Applied Catalysis B: Environmental 162 (2015) 174–179

Contents lists available at ScienceDirect

Applied Catalysis B: Environmental

journal homepage: www.elsevier.com/locate/apcatb

Formation of reactive Lewis acid sites on Fe/WO_3–ZrO_2 catalysts for higher temperature SCR applications

Rodney Foo[a,1], Tanya Vazhnova[a], Dmitry B. Lukyanov[a], Paul Millington[b], Jillian Collier[b], Raj Rajaram[b], Stan Golunski[c,*]

[a] Catalysis and Reaction Engineering Group, Department of Chemical Engineering, University of Bath, Bath BA2 7AY, UK
[b] Johnson Matthey Technology Centre, Blount's Court, Sonning Common, Reading RG4 9NH, UK
[c] Cardiff Catalysis Institute, School of Chemistry, Cardiff University, Main Building, Cardiff CF10 3AT, UK

ARTICLE INFO

Article history:
Received 5 May 2014
Received in revised form 11 June 2014
Accepted 19 June 2014
Available online 26 June 2014

Keywords:
Selective catalytic reduction
Nitrogen oxide
Iron
Tungsten zirconia
Acidity

ABSTRACT

Tungsten–zirconia (WO_3–ZrO_2), which oxidises NH_3 but shows no NO_x-reduction activity, can be converted into an active ammonia-SCR catalyst by impregnation with Fe. The role of Fe in inducing SCR activity has been studied by relating the catalytic performance of tungsten–zirconia materials (containing 0, 0.5, 2, 3 and 10 wt% Fe) to their surface acidity, which has been probed by pyridine adsorption. The most active material, 3 wt% Fe/WO_3–ZrO_2, reduces NO_x by 10-20% at the minimum temperature tested (150 °C), and achieves 80–85% conversion at temperatures between 400 and 550 °C. The performance can be correlated with the formation of new Fe^{3+} Lewis acid sites that have a pivotal role in the SCR reaction by activating NO_x, and which are associated with a characteristic peak shift in the IR spectrum of adsorbed pyridine. The introduction of Fe also has the effect of increasing the strength of the Brønsted acidity, which accounts for the similarity in activity observed between the Fe/WO_3–ZrO_2 materials and benchmark Fe/beta-zeolite catalysts at higher temperatures.

1. Introduction

Selective catalytic reduction (SCR) of nitrogen oxides (NO_x) by ammonia is a proven technology for reducing NO_x emissions in flue gases from stationary sources. Current industrial catalysts for this application are generally still based on V_2O_5, which is usually promoted with WO_3, supported on TiO_2, and stabilised with siliceous materials [1]. The same formulation can be used for NO_x control on diesel vehicles, where ammonia is generated in-situ by the hydrolysis of urea [2]. However, many after treatment systems now combine SCR catalysis with soot filtration in an integrated unit, in which high temperatures are intermittently induced in order to regenerate the filter [3]. Under these very demanding conditions, V_2O_5 catalysts do not show the long-term durability that is legally required of after treatment systems throughout the world, but there is only a limited 'toolkit' of alternative catalyst components that can deliver the target activity and selectivity. These include Fe, Mn, Cu and Ce as the active metal oxides [4–6], and beta-zeolite, ZSM-5, SAPO-34, and acidic metal oxides as the supports [7–10]. Although currently the best performance can be achieved by Cu- and Fe-exchanged small-pore zeotype materials [11], stable metal oxide supports are still being evaluated as alternatives, particularly for heavy-duty applications in which the catalysts can operate for extended periods at temperatures between 250 °C and 450 °C. Without the active-site protection from gas-phase inhibitors and poisons that small-pore zeotype materials can provide, though, the choice of catalyst components becomes very limited.

Ever since the pioneering work of Hino and Arata [12], there has been considerable interest in tungstate- and sulphate-doped zirconia as acidic supports. In particular, sulphated zirconia can be widely used catalytically, but it suffers from poor thermal stability due to the loss of sulphate groups [13–15]. The more stable tungsten zirconia [16–19] has therefore been increasingly seen as a potential catalyst or support, particularly in such applications as hydrocarbon isomerisation and alkylation reactions [20–23]. Over the same period, iron based materials including Fe supported on pillared clays [24], mixed oxides [25,26] and particularly zeolites [27–34] have emerged as active ammonia-SCR catalysts. An overview of the scientific literature from the past 10 years (such as the work of Kureti and co-workers [35]) suggests that a combination of

* Corresponding author. Tel.: +44 0 2920870826.
E-mail address: golunskise@cardiff.ac.uk (S. Golunski).
[1] Present address: BP Global Fuels Technology, Technology Centre, Pangbourne, Reading RG8 7QR, UK.

http://dx.doi.org/10.1016/j.apcatb.2014.06.034
0926-3373/

tungsten–zirconia, as a catalyst support, with iron oxide, as the active metal oxide, is a system that could be optimised to achieve high activity and longevity during operation at moderate-to-high temperatures. In this study, we show how a relatively subtle change in the nature of the surface Lewis acidity can have a marked effect on the activity of this largely overlooked catalyst system. When considered in the context of other published work in this field, the results indicate that there are certain generic similarities between many ammonia-SCR catalysts, despite marked differences in their compositions. Furthermore, we have seen that the adsorption of a common probe molecule (pyridine) can be correlated with SCR activity, suggesting that this familiar technique could be used to predict the SCR performance of new catalyst formulations, and to establish the extent of deactivation of engine-aged catalysts.

2. Experimental

As the catalytic properties of Fe/beta-zeolite are among the best understood in the field of ammonia-SCR, it is often used as a reference material for assessing other potential catalysts [27,36,37]. Therefore, in this study, we have used two specific Fe/beta-zeolite formulations as benchmarks against which to rank the activity of a range of Fe on tungsten–zirconia materials.

2.1. Catalyst preparation and ageing

Commercially available tungsten–zirconia (DKK; 9 wt% WO_3–ZrO_2) and beta zeolite (Zeolyst; $SiO_2/Al_2O_3 = 75$) were used as the catalyst supports. Both materials were dried at 60 °C for 24 h, and the tungsten–zirconia was subsequently calcined at 830 °C. The catalysts were prepared by impregnation to incipient wetness, using aqueous solutions of iron nitrate nonahydrate (Fluka; $Fe(NO_3)_3{\cdot}9H_2O$). After impregnation, the samples were calcined at 600 °C in a continuous flow of dry air. The nominal content of iron in the beta-zeolite catalysts was 0.5 and 2 wt%; these are referred to as 0.5Fe/beta and 2Fe/beta catalysts, respectively. Four non-zeolite iron materials were prepared with nominal metal loadings of 0.5, 2, 3 and 10 wt%; these are referred to as *x*Fe/WO_3–ZrO_2, where *x* indicates the Fe loading (wt%).

In our durability trials, fresh samples of the Fe/beta-zeolite catalysts and Fe/WO_3–ZrO_2 materials were hydrothermally aged (10 mol% steam in flowing air; 700 °C) for 65 h before being tested.

2.2. Surface characterisation

The BET surface areas of the WO_3–ZrO_2 support and the Fe/WO_3–ZrO_2 materials were measured using a Micrometrics ASAP 2010 instrument, after degassing the samples at 250 °C.

The concentrations of Brønsted acid sites (BAS) and Lewis acid sites (LAS) were determined by in situ Fourier transform infrared (FT-IR) spectroscopy, with pyridine as the probe molecule. These studies were carried out using a Bruker Equinox 55 FT-IR spectrometer at a resolution of 2 cm^{-1}. The samples were pressed into self supported discs weighing 10–20 mg that were placed in the sample holder. The samples were then heated from room temperature to 350 °C at a rate of 1 °C min^{-1} under vacuum. The samples were held at 350 °C for 2 h and then cooled to 100 °C. To measure the total acidity, pyridine was introduced into the IR-cell in 0.02 μL increments until the sample was saturated, and the IR spectra were taken after each pyridine injection. From the individual peak intensities, the amount of pyridine adsorbed at each type of acid site could be calculated, providing a direct measure of the acid site concentration (in μmol g^{-1}). The concentration of residual surface pyridine was subsequently determined during thermal desorption, by heating the sample to 200, 250, 300 and 350 °C, and recording spectra after dwelling at each temperature for 30 min.

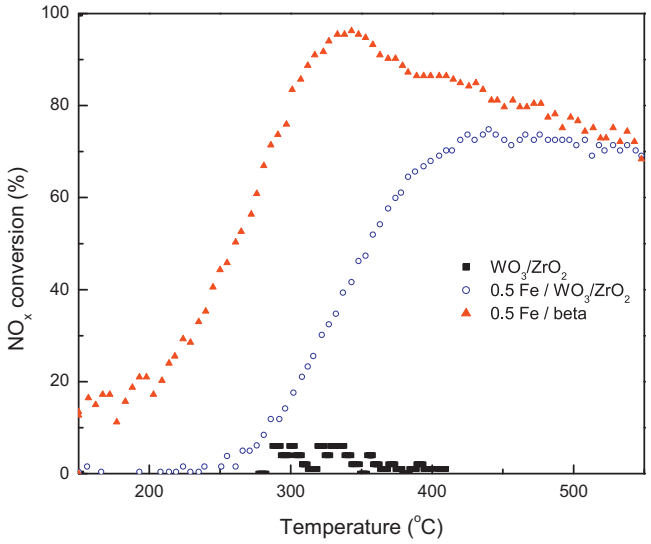

Fig. 1. Effect of temperature on NO_x conversion to N_2 over WO_3–ZrO_2, 0.5Fe/WO_3–ZrO_2 and 0.5Fe/beta-zeolite.

2.3. Catalytic studies

The selective catalytic reduction of NO_x by NH_3 was studied in a fixed-bed continuous flow reactor, under conditions (gas composition, temperature range and space velocity) that were intended to mimic those in the tailpipe of a diesel vehicle running on sulphur-free fuel. The catalysts were pressed into pellets, crushed and sieved to a mesh size of 250–350 μm, then loaded into an inconel 8 mm ID reactor and fixed in place with quartz wool. Each catalyst charge (0.3 g) was heated from 150 to 600 °C at a rate of 5 °C min^{-1} in a reactant mixture of 12 mol% O_2, 5% CO_2, 10% H_2O (steam), 100 mol-ppm NH_3 and 100 ppm NO in nitrogen at a total flow rate of 2 L min^{-1}. A blank test with a cordierite charge, instead of catalyst, was run before each series of samples was tested. The downstream concentrations of NO, total NO_x and NH_3 were measured using a chemiluminescent analyser (Signal Instruments 4000VM), while a multi-gas analyser (ADC MGA-3000 series) was used to detect the formation of any N_2O.

In comparing catalytic activity, we use a notation that is conventional in after treatment catalysis, whereby T_{10} and T_{50} indicate the temperatures at which the NO concentration is reduced by 10% and 50%, respectively.

3. Results and discussion

3.1. Catalytic activity

As expected, the tungsten–zirconia support (without iron) had minimal activity for ammonia-SCR under simulated diesel exhaust conditions, over the entire temperature range tested (Fig. 1). However, even the addition of a small amount of iron (0.5 wt%) had a pronounced effect on NO_x reduction to N_2, particularly at the highest temperatures (450–550 °C) where the activity was now similar to that of the benchmark Fe/beta-zeolite catalyst with a comparable Fe loading. At lower temperatures, 0.5Fe/WO_3–ZrO_2 still showed very poor activity (T_{10} = 300 °C; T_{50} = 360 °C) compared to 0.5Fe/beta-zeolite (T_{10} < 150 °C; T_{50} = 250 °C) which achieved 95% NO_x conversion at 330 °C. Significantly, there was a clear lag between the onset of the NO_x-reduction curve and the onset of the

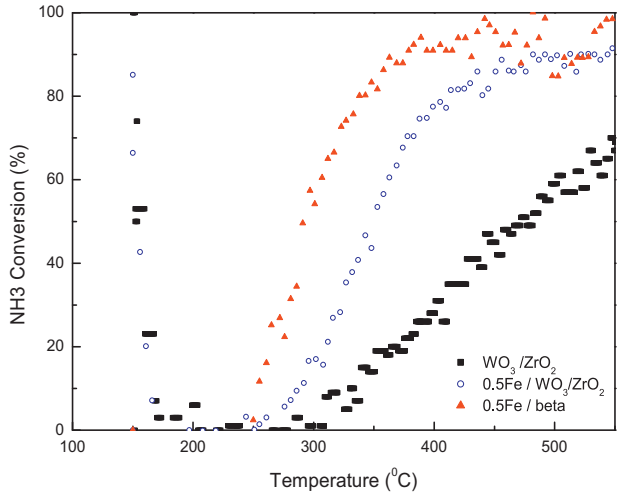

Fig. 2. Effect of temperature on NH_3 conversion over WO_3–ZrO_2, 0.5Fe/WO_3–ZrO_2 and 0.5Fe/beta-zeolite.

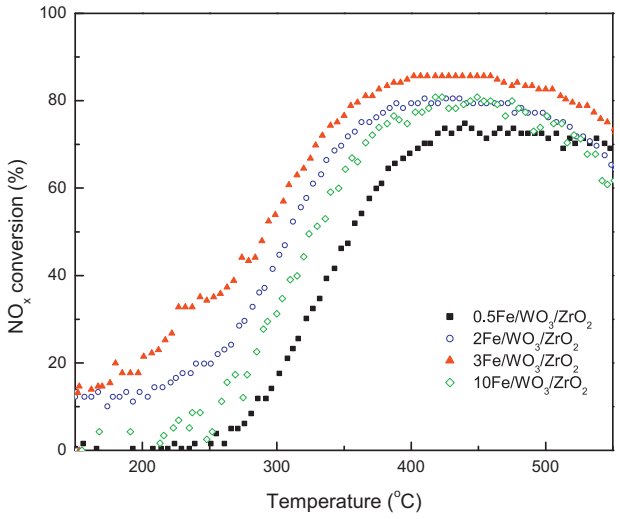

Fig. 3. Effect of temperature on NO_x conversion to N_2 over four Fe/WO_3–ZrO_2 catalysts with different iron loadings.

ammonia-conversion curve for both the Fe/beta-zeolites (e.g. compare 0.5Fe/beta-zeolite in Figs. 1 and 2) and for the 2Fe/WO_3–ZrO_2 and 3Fe/WO_3–ZrO_2 materials. Key to understanding this lag is the fact that the first event that we invariably observed, as soon as the NH_3-containing simulated exhaust gas initially came into contact with the catalyst bed, was a large spike in apparent NH_3 conversion. (The tail of this spike can be clearly seen between 150 and 170 °C for the WO_3–ZrO_2 and 0.5Fe/WO_3–ZrO_2 in Fig. 2.) This apparent conversion of NH_3 was due to its adsorption at acid sites, which rapidly became saturated. The initial phase of NO_x reduction (below ca 250 °C) cannot be attributed to reaction with the pre-adsorbed NH_3 by the type of Eley-Rideal mechanism proposed by several authors in the past (e.g. see review by Li et al. [10]), because WO_3–ZrO_2 showed no low-temperature SCR activity despite a high NH_3-adsorption capacity. Only with the addition of at least 2 wt% Fe did the low-temperature activity start to become apparent.

Another distinctive feature of the SCR activity of the benchmark 0.5Fe/beta-zeolite was the inversion in NO_x-reduction above 330 °C, which led to its activity converging with that of 0.5Fe/WO_3–ZrO_2 at the highest temperatures. The associated NH_3 conversion plot for 0.5Fe/beta-zeolite (Fig. 2) shows a continuing rise above 330 °C, indicating that the inversion in NO_x-reduction arises from the non-selective combustion of ammonia (Eq. (1)). It is also notable that ammonia conversion exceeded the 1:1 stoichiometry expected for the SCR reaction (Eq. (2)) across the whole temperature range over which 0.5Fe/WO_3–ZrO_2 was active for NO_x reduction, but this was not the case for the higher loaded materials. As Fe-free WO_3/ZrO_2 was also capable of converting ammonia, and it did so without generating NO_x, we conclude that the major non-selective reaction over WO_3–ZrO_2 and 0.5Fe/WO_3–ZrO_2 was the partial oxidation of NH_3 to N_2 and H_2O (Eq. (3)).

$$\text{Non-selective combustion} \quad 4NH_3 + 7O_2 \rightarrow 4NO_2 + 3H_2O \ldots \quad (1)$$

$$\text{Selective reduction} \quad 4NH_3 + 4NO + O_2 \rightarrow 4N_2 + 6H_2O \ldots \quad (2)$$

$$\text{Non-selective partial oxidation} \quad 4NH_3 + 3O_2 \rightarrow 2N_2 + 6H_2O \ldots \quad (3)$$

A substantial improvement in NO_x reduction was observed over the entire temperature range when the iron loading was increased from 0.5% to 2% on the tungsten–zirconia (Fig. 3). This was reflected in a decrease in the T_{10} temperature by 150 °C, and in the T_{50} temperature by 35 °C. Addition of another 1% Fe (to 3%) further improved the activity, but the magnitude suggested that we were now close to the optimum loading. A further large increment in Fe loading (to 10%) resulted in a decline in overall activity compared to 3Fe/WO_3–ZrO_2, though it was still higher than that of 0.5Fe/WO_3–ZrO_2 (except close to the maximum temperature). The improvement in the SCR activity as the loading was increased from 0.5 to 3 wt% is consistent with the formation of a larger number of mononuclear Fe sites. From detailed characterisation of Fe/ZSM-5, it has been reported that mononuclear Fe provides the active sites for NO_x reduction [32]. However, at loadings above 3 wt% Fe in the zeolite, bulk iron species are expected to form, and these iron clusters have been shown to be unselective [30,38].

3.2. Surface acidity

Fig. 4 shows the pyridine-adsorption (Py) region of the IR spectra for WO_3–ZrO_2, 0.5Fe/WO_3–ZrO_2 and 2Fe/WO_3–ZrO_2, after subtraction of the baseline for the three materials (i.e. before pyridine

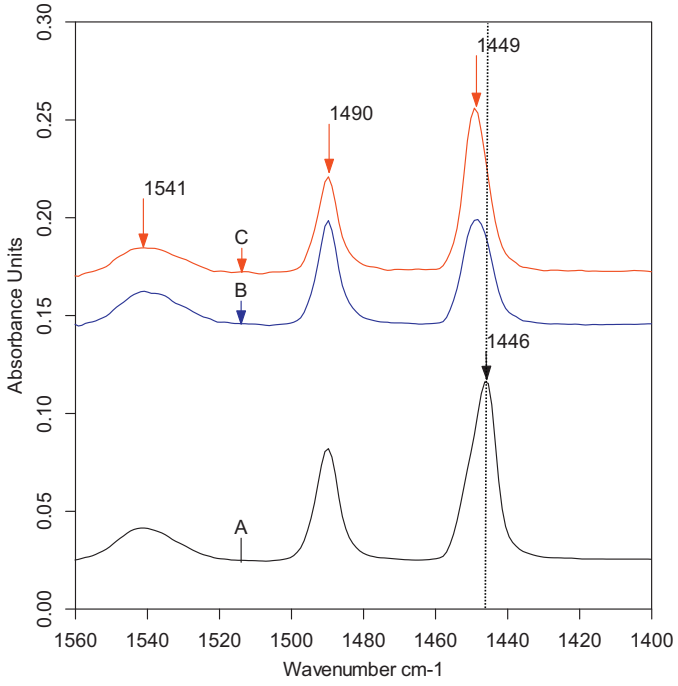

Fig. 4. Weight-normalised IR spectra (Py region) of (A) WO_3–ZrO_2, (B) 0.5Fe/WO_3–ZrO_2 and (C) 2Fe/WO_3–ZrO_2.

Table 1
Surface characterisation of tungsten–zirconia materials: (i) BET surface area, and (ii) concentration of LAS and BAS, as determined by pyridine adsorption. The IR position of each Py-LAS and Py-BAS peak is shown in brackets. The benchmark 2Fe/beta-zeolite catalyst is included for comparison.

	BET-SA ($m^2\,g^{-1}$)	[LAS] ($\mu mol\,g^{-1}$)	[BAS] ($\mu mol\,g^{-1}$)
WO_3/ZrO_2	143	31 (1446 cm^{-1})	12.4 (1541 cm^{-1})
$0.5Fe/WO_3–ZrO_2$	148	18.6 (1449 cm^{-1})	12.4 (1541 cm^{-1})
$2Fe/WO_3–ZrO_2$	178	26.8 (1449 cm^{-1})	6.0 (1541 cm^{-1})
2Fe/beta-zeolite	–	130.2 (1450 cm^{-1})	55.8 (1547 cm^{-1})

adsorption). Based on interpretations in the literature [39,40], the IR peaks can be assigned to pyridine adsorbed on both Brønsted and Lewis acid sites: 1541 cm^{-1} (BAS), 1490 cm^{-1} (either BAS or LAS), and 1446 cm^{-1} (LAS). The intensity of each peak was directly proportional to the concentration ($\mu mol\,g^{-1}$) of the specific type of surface acid site.

The most notable effect of adding iron to $WO_3–ZrO_2$ was that the intensity of the unambiguous 1446 cm^{-1} peak, associated with pyridine on LAS (Py-LAS) [41], decreased by ~40% and its position shifted to a higher wavenumber (Table 1). The intensity of the shifted peak (now at 1449 cm^{-1}) increased as the Fe-loading was raised to 2%. At the same time, the intensity of the other unambiguous peak (Py-BAS at 1541 cm^{-1}) was the same for both $WO_3–ZrO_2$ and $0.5Fe/WO_3–ZrO_2$, before a 20% reduction was observed in the $2Fe/WO_3–ZrO_2$ material (Table 1). By analogy to the effect of adding Fe to sulphated ZrO_2 [42,43], we attribute the changes in the Py-LAS peak to the blocking of one type of Lewis acidity as new LAS are created. We also observed a change in Lewis acidity on addition of Fe to H/beta-zeolite, though here the Py-LAS peak (at 1456 cm^{-1}) was shifted to a lower wavenumber (1450 cm^{-1} for Fe/beta) while increasing in intensity (Fig. 5). We propose, therefore, that it is these new LAS that are responsible for inducing SCR activity when Fe is added to an acidic support material with little or no intrinsic activity for NO_x reduction (see below for more detail). The pyridine-retention profiles (Fig. 6) show that the strength of both the BAS and LAS are enhanced when iron is introduced, consistent with previous reports [18].

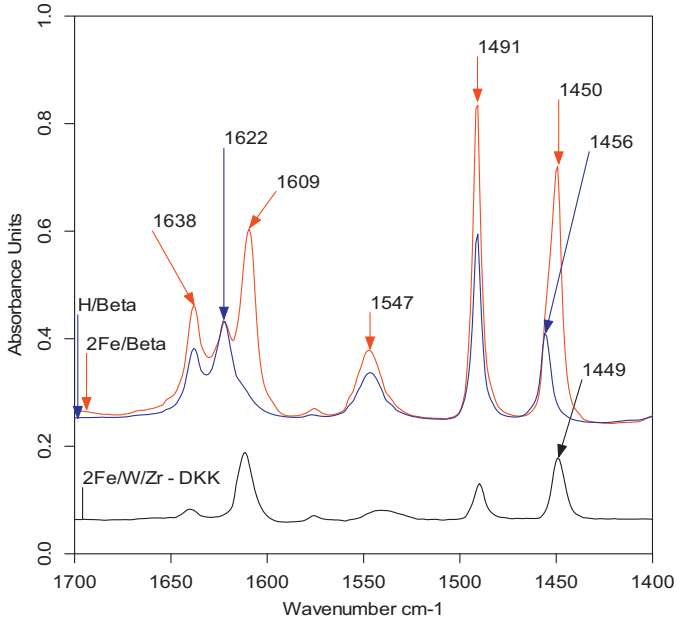

Fig. 5. Weight-normalised IR spectra (Py region) of H/beta, 2Fe/beta and $2Fe/WO_3–ZrO_2$.

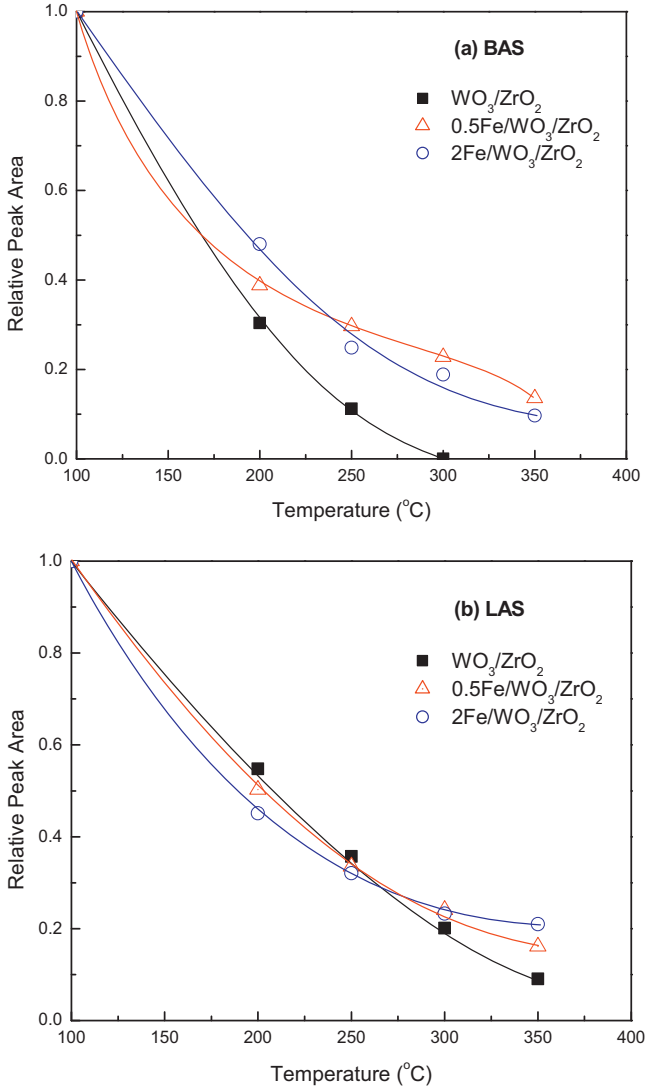

Fig. 6. Effect of temperature on pyridine retention on (a) BAS and (b) LAS present in $WO_3–ZrO_2$, $0.5Fe/WO_3–ZrO_2$ and $2Fe/WO_3–ZrO_2$.

3.3. Acidity–activity correlation

As mentioned above, convincing evidence already exists [42,43] for the role of iron in generating new LAS when introduced into an acidic zirconia-based isomerisation catalyst. We conclude that there is a similar transformation in the surface acidity of tungsten–zirconia when iron is added, as characterised by the small but definite peak shift from 1446 cm^{-1} to 1449 cm^{-1} in the IR spectrum of adsorbed pyridine. Furthermore, the new LAS have higher acid strength, as shown by pyridine-retention as a function of temperature (Fig. 6).

The LAS on tungsten–zirconia are generally attributed to free Zr^{4+} sites that are not occupied by tungstate species, whereas the BAS are associated with polytungstate clusters on zirconia [16,44–46]. When zirconium oxide is impregnated with tungsten, the tungstate species 'consume' the zirconium-LAS, generating new BAS [44,47]. As there is a strong iron–zirconia interaction [48], it is likely that iron will preferentially interact with any remaining free Zr^{4+} sites instead of with the tungstate species. Our results (in Table 1) support this model, as the number of LAS is reduced initially as Fe is introduced, before any change in the number of BAS is detected. Therefore, as the Fe species occupy the Zr^{4+} sites associated with the Py-LAS peak at 1446 cm^{-1}, a smaller number of new

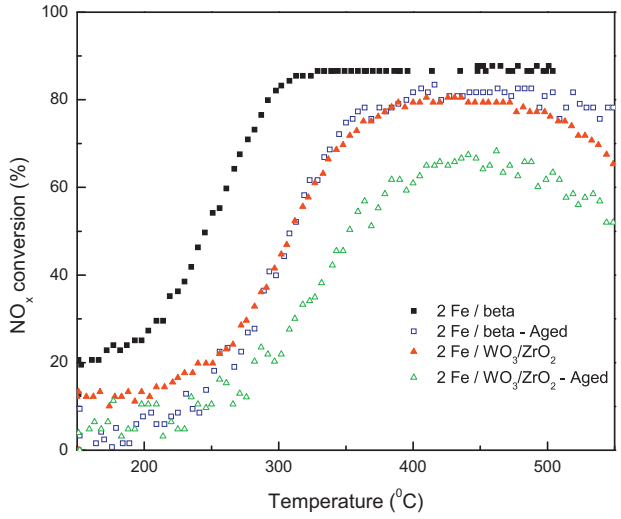

Fig. 7. Effect of temperature on NO_x conversion to N_2 over fresh and aged $2Fe/WO_3–ZrO_2$ and 2Fe/beta-zeolite.

Fe^{3+} LAS (1449 cm^{-1}) are created, but these are critical to the ability of the material to achieve high NO_x reduction. We suggest that the new LAS are responsible for NO activation on the catalyst surface, enabling the SCR reaction to take place predominantly through a Langmuir-Hinshelwood mechanism. On increasing the iron loading from 0.5 to 3 wt%, more of these LAS are generated, which in turn result in an increase in the overall catalytic activity. Similar Fe^{3+} LAS are present in the benchmark Fe/beta-zeolite catalysts, but at much higher concentrations. For example, the surface concentration of Fe^{3+} LAS in $2Fe/WO_3–ZrO_2$ was 26.8 μmol g^{-1}, whereas the concentration in 2Fe/beta-zeolite was 130.2 μmol g^{-1} (Table 1).

Finally, let us consider the effect of iron loading on the number of BAS in the $Fe/WO_3–ZrO_2$ catalysts. These sites are responsible for the strong adsorption of NH_3 to form the surface NH_4^+ species that can determine the upper temperature limit for NO_x-reduction, but may also account for the oxidation of NH_3 at higher temperatures [49]. Initially, at low Fe loading, there is no change in the number of BAS. However, at higher loadings, a drop in the number of BAS is observed (Table 1). This is likely to take place once all the free Zr^{4+} sites are occupied by Fe species. This could be due either to the excess iron interacting directly with tungsten species or aggregating into larger clusters. Such Fe clusters may then interact with nearby WO_3 species, with this interaction being strong enough to cause a decrease in the number of BAS. This perturbation of the tungsten–zirconia interactions caused by Fe species occupying nearby Zr^{4+} LAS could also lead to the observed increase in BAS strength. Again, analogous BAS sites are present at much higher concentrations in the benchmark Fe/beta-zeolite catalysts (55.8 μmol g^{-1} in 2Fe/beta-zeolite compared to 6 μmol g^{-1} in $2Fe/WO_3–ZrO_2$).

3.4. Hydrothermal durability

Although the activity of SCR catalysts can be inhibited by carbon deposition and by the presence of gas-phase SO_2, the major cause of irreversible deactivation of many metal-exchanged zeolite catalysts is through hydrothermally induced de-alumination of the zeolite structure [10]. Replacing beta-zeolite by a more durable acidic support material would, therefore, be expected to increase the longevity of Fe-based SCR catalysts.

After severe hydrothermal ageing, both the Fe/beta-zeolite catalysts and the $Fe/WO_3–ZrO_2$ materials showed stable but depressed activity. For brevity, Fig. 7 compares only the fresh and aged performance of $2Fe/WO_3–ZrO_2$ with that of 2Fe/beta-zeolite, since similar trends were observed for the other pairs of samples. A substantial drop in the catalytic activity of the 2Fe/beta-zeolite catalyst is seen in the low temperature region (<300 °C) after ageing, but the peak activity has remained comparable to that of the fresh catalyst. A much smaller decrease in the low-temperature activity was observed after ageing the $2Fe/WO_3–ZrO_2$ material, reflecting a proportionally smaller decrease in the pre-adsorption of NH_3 that leads to initial NO_x reduction. A key effect of ageing 2Fe/beta-zeolite catalyst is a narrowing of the window for maximum NO_x reduction, so that it resembles (in width and shape) the activity window for fresh and aged $2Fe/WO_3–ZrO_2$. It is interesting that the NO_x-reduction trace for aged 2Fe/beta-zeolite can be almost entirely superimposed over the trace for fresh $2Fe/WO_3–ZrO_2$. We expect that this convergence in performance can be tracked by the change in surface concentration of the acid sites, primarily the LAS, which we expect to confirm and model in the future.

4. Conclusions

Tungsten–zirconia is an established acid catalyst for hydrocarbon isomerisation reactions [20], and a potential alternative to small-pore zeotype materials as an acidic support for ammonia-SCR catalysts [35]. The nature of its acidity is known to change when it is impregnated with Fe, often resulting in a switchover from BAS to LAS as the predominant acid sites [44]. Whereas this has an adverse effect on isomerisation activity [43], the addition of Fe is essential to ammonia-SCR activity, with negligible NO_x conversion being observed over tungsten–zirconia alone.

Our work shows that the change in Brønsted/Lewis acid-site ratio is not the underlying cause of ammonia-SCR activity, when Fe is added to tungsten–zirconia. Instead, the critical function of Fe is to transform one type of LAS into reactive sites. This transformation can be tracked by a shift in the characteristic IR peak position for pyridine adsorbed on the LAS, which is diagnostic of the formation of the new Fe acid sites that instil NO_x-reduction activity. (This is very similar to the effect of Fe on beta-zeolite, where the creation of the reactive sites has been tracked by a characteristic ESR signal [7].) As tungsten–zirconia already has a high capacity for storing ammonia, the creation of the new sites must be pivotal to the activation of NO. To explain the resultant enhancement in NO_x reduction, we favour a Langmuir–Hinshelwood mechanism (of the type proposed by Liu et al. [34]) in which NO is adsorbed oxidatively at the new sites, while the other LAS and BAS adsorb NH_3 to form a reservoir of available reductant. Furthermore, the sustained NO_x-reduction activity at relatively high temperature (500 °C) reflects the enhanced strength of all the acid sites when Fe is present.

The results of this study highlight features that are common to several ammonia-SCR catalysts, despite major differences in composition. When the active metal phase is either Cu or Fe, the pivotal sites are isolated metal ions in a high oxidation state, i.e. Cu^{2+} [9] and Fe^{3+} [7], irrespective of whether the support is a zeotype or an acidic metal oxide material. The metal ion sites are pivotal because, in their absence, the support materials are capable of adsorbing NH_3, but are not able to activate sufficient NO to enable substantial SCR activity through a Langmuir–Hinshelwood pathway. Although various techniques can be used to detect these sites [7,9], our work shows that pyridine adsorption is particularly informative both in tracking their formation and in identifying their Lewis acid character.

Acknowledgements

This work was funded by Johnson Matthey PLC and the Department of Chemical Engineering at the University of Bath.

References

[1] K. Skalska, J.S. Miller, S. Ledakowicz, Sci. Total Environ. 408 (2010) 3976–3989.
[2] A.M. Bernhard, D. Peitz, M. Elsener, T. Schildhauer, O. Krocher, Catal. Sci. Technol. 3 (2013) 942–951.
[3] G. Cavataio, J. Girard, J.E. Patterson, C. Montreuil, Y. Cheng, C.K. Lambert, SAE Tech. Pap. Series (2007), 2007-01-1575.
[4] J.M. Fedeyko, B. Chen, H.-Y. Chen, Catal. Today 151 (2010) 231–236.
[5] G.S. Qi, R.T. Yang, R. Chang, Appl. Catal., B: Environ. 51 (2004) 93-.
[6] L. Chen, D. Weng, Z. Si, X. Wu, Prog. Nat. Sci.: Mater. Int. 22 (2012) 265–272.
[7] D.E. Doronkin, A.Y. Stakheev, A.V. Kucherov, N.N. Tolkachev, G.O. Bragina, G.N. Baeva, P. Gabrielsson, I. Gekas, S. Dahl, Mendeleev Commun. 17 (2007) 309–310.
[8] S. Brandenberger, O. Krocher, A. Wokaun, A. Tissler, R. Althoff, J. Catal. 268 (2009) 297–306.
[9] J. Xue, X. Wang, G. Qi, J. Wang, M. Shen, W. Li, J. Catal. 297 (2013) 56–64.
[10] J. Li, H. Chang, L. Ma, R.T. Yang, Catal. Today 175 (2011) 147–156.
[11] P.S. Metkar, M.P. Harold, V. Balakotaiah, Chem. Eng. Sci. 87 (2013) 51–66.
[12] M. Hino, K. Arata, Chem. Commun. (1987) 1259–1260.
[13] F.T.T. Ng, N. Horvat, Appl. Catal., A: Gen. 123 (1995) L197–L203.
[14] F.R. Chen, G. Coudurier, J.F. Joly, J.C. Vedrine, J. Catal. 143 (1993) 616–626.
[15] R. Srinivasan, R.A. Keogh, D.R. Milburn, B.H. Davis, J. Catal. 153 (1995) 123–130.
[16] D.G. Barton, S.L. Soled, G.D. Meitzner, G.A. Fuentes, E. Iglesia, J. Catal. 181 (1999) 57–72.
[17] K. Arata, Appl. Catal., A: Gen. 146 (1996) 3–32.
[18] J.C. Vartuli, J.G. Santiesteban, P. Traverso, N. Cardona-Martinez, C.D. Chang, S.A. Stevenson, J. Catal. 187 (1999) 131–138.
[19] K. Shimizu, T.N. Venkatraman, W. Song, Appl. Catal., A: Gen. 224 (2002) 77–87.
[20] S. De Rossi, G. Ferraris, M. Valigi, D. Gazzoli, Appl. Catal., A: Gen. 231 (2002) 173–184.
[21] J.G. Santiesteban, J.C. Vartuli, S. Han, R.D. Bastian, C.D. Chang, J. Catal. 168 (1997) 431–441.
[22] S. Kuba, P. Lukinskas, R.K. Grasselli, B.C. Gates, H. Knozinger, J. Catal. 216 (2003) 353–361.
[23] T. Li, S.T. Wong, M.C. Chao, H.P. Lin, C.Y. Mou, S. Cheng, Appl. Catal., A: Gen. 261 (2004) 211–219.
[24] R.Q. Long, R.T. Yang, Appl. Cat., B: Environ. 27 (2000) 87–95.
[25] G. Ramis, L. Yi, G. Busca, M. Turco, E. Kotur, R.J. Willey, J. Catal. 157 (1995) 523–535.
[26] R.J. Willey, H. Lai, J.B. Peri, J. Catal. 130 (1991) 319–331.
[27] R.Q. Long, R.T. Yang, J. Catal. 207 (2002) 274–285.
[28] G. Delahay, M. Mauvezin, B. Coq, S. Kieger, J. Catal. 202 (2001) 156–162.
[29] H. Sjovall, L. Olsson, E. Fridell, R.J. Blint, Appl. Cat., B: Environ. 64 (2006) 180–188.
[30] M.S. Kumar, M. Schwidder, W. Grunert, A. Bruckner, J. Catal. 227 (2004) 384–397.
[31] G. Qi, R.T. Yang, Appl. Cat., B: Environ. 60 (2005) 13–22.
[32] M. Schwidder, M.S. Kumar, K. Klementiev, M.M. Pohl, A. Bruckner, W. Grunert, J. Catal. 231 (2005) 314–330.
[33] G. Delahay, D. Valade, A. Guzman-Vargas, B. Coq, Appl. Cat., B: Environ. 55 (2005) 149–155.
[34] Z. Liu, P.J. Millington, J.E. Bailie, R.R. Rajaram, J.A. Anderson, Microporous Mesoporous Mater. 104 (2007) 159–170.
[35] N. Apostolescu, B. Geiger, K. Hizbullah, M.T. Jan, S. Kureti, D. Reichert, F. Schott, W. Weisweiler, Appl. Cat., B: Environ. 62 (2006) 104–114.
[36] B. Coq, M. Mauvezin, G. Delahay, J.-B. Butet, S. Kieger, Appl. Catal., B: Environ. 27 (2000) 193–198.
[37] K. Rahkamaa-Tolonen, T. Maunula, M. Lomma, M. Huuhtanen, R.L. Keiski, Catal. Today 100 (2005) 217–222.
[38] M. Scheithauer, E. Bosch, U.A. Schubert, H. Knozinger, T.K. Cheung, F.C. Jentoft, B.C. Gates, B. Tesche, J. Catal. 177 (1998) 137–146.
[39] E.P. Parry, J. Catal. 2 (1963) 371–379.
[40] G. Busca, Phys. Chem. Chem. Phys. 1 (1999) 723–736.
[41] M.-T. Tran, N.S. Gnep, G. Szabo, M. Guisnet, Appl. Catal., A: Gen. 171 (1998) 207–217.
[42] F.C. Jentoft, A. Hahn, J. Krohnert, G. Lorenz, R.E. Jentoft, T. Ressler, U. Wild, R. Schlogl, C. Hassner, K. Kohler, J. Catal. 224 (2004) 124–137.
[43] T. Loften, N.S. Gnep, M. Guisnet, E.A. Blekkan, Catal. Today 100 (2005) 397–401.
[44] M. Scheithauer, T.K. Cheung, R.E. Jentoft, R.K. Grasselli, B.C. Gates, H. Knozinger, J. Catal. 180 (1998) 1–13.
[45] C.D. Baertsch, S.L. Soled, E. Iglesia, J. Phys. Chem. B 105 (2001) 1320–1330.
[46] C.D. Baertsch, K.T. Komala, Y.-H. Chua, E. Iglesia, J. Catal. 205 (2002) 44–57.
[47] T.N. Vu, J. van Gestel, J.P. Gilson, C. Collet, J.P. Dath, J.C. Duchet, J. Catal. 231 (2005) 453–467.
[48] E. Guglielminotti, J. Phys. Chem. 98 (1994) 4884–4891.
[49] X. Chen, W. Li, J. Schwank, Catal. Today 175 (2011) 2–11.